

REVIEW

Energy storage devices in electrified railway systems: A review

Xuan Liu and Kang Li*

University of Leeds, School of Electronics and Electrical Engineering, Leeds, LS2 9JL, UK

*Corresponding author. E-mail: k.li1@leeds.ac.uk

Abstract

As a large energy consumer, the railway systems in many countries have been electrified gradually for the purposes of performance improvement and emission reduction. With the widespread utilization of energy-saving technologies such as regenerative braking techniques, and in support of the full electrification of railway systems in a wide range of application conditions, energy storage systems (ESSes) have come to play an essential role. In this paper, some recent developments in railway ESSes are reviewed and a comprehensive comparison is presented for various ESS technologies. The foremost functionalities of the railway ESSes are presented together with possible solutions proposed from the academic arena and current practice in the railway industry. In addition, the challenges and future trends of ESSes in the railway industry are briefly discussed.

Keywords: energy storage; railway system; regenerative energy

1. Introduction

Climate change and environmental sustainability have drawn substantial worldwide public attention in the past decade. The importance of the widespread utilization of clean energy has become increasingly prominent. As one of the largest energy consumers, transportation has been moving towards electrification, since electrical energy provides a number of environmental benefits due to the significant uptake of renewable energies

in electric power systems. Electrified railway systems not only reduce carbon dioxide emissions [1] but also enhance the performance of the vehicles [2]. Nowadays, there is a growing interest in improving the energy efficiency of railway vehicles; in particular, braking energy recovery has drawn substantial attention. Due to the widespread utilization of regenerative braking technologies, electric railway vehicles are able to convert the kinetic energy (in the braking phase) into electric energy for the purpose of energy

Received: 29 March 2020; Revised: 16 May 2020; Accepted: 3 June 2020

© The Author(s) 2020. Published by Oxford University Press on behalf of Central South University Press. This is an Open Access article distributed under the terms of the Creative Commons Attribution License (<http://creativecommons.org/licenses/by/4.0/>), which permits unrestricted reuse, distribution, and reproduction in any medium, provided the original work is properly cited.

reuse. Generally, there are three solutions to manage regenerative braking energy (RBE) in railway vehicles:

- (i) Synchronizing the loads along the traction power supply lines;
- (ii) Feeding the RBE back to the external grid; and
- (iii) Storing the RBE in an ESS.

The RBE can be used by other railway vehicles. This solution not only enhances energy efficiency but also reduces the peak power demand from the railway. Therefore, the synchronization of the presence of RBE and traction power is necessary. Optimization of railway timetables [3–5] and driving strategies [6–8] are widely studied to enhance such synchronization. However, the schedule and operation performance of the railway vehicles are constrained by the transport market and safety regulations, which makes the optimization very complicated and challenging.

Feeding the RBE to the external grid (e.g. the upstream AC grid) via the substations is another solution. For DC railway lines, this approach is implemented based on reversible substations which allow current to flow bidirectionally through the use of power electronics inverters. However, if the reversible substation cannot provide an acceptable level of power quality, harmonics pollution from the traction systems may be passed on to the external grid [9]. Moreover, this approach also faces the challenges of cost, complexity and scalability for widespread adoption [10].

Due to the rapid developments of power electronics and energy-storage technologies, the utilization of ESSes in railway networks stands out as an alternative approach to overcome the drawbacks of the aforementioned solutions. Unlike techniques that transmit RBE to other loads or feed RBE back to the external grid, this approach stores RBE in ESSes for later use. The installation of ESSes can be either stationary or on-board, depending on the demanded functionalities of the ESS. A comparison between stationary and on-board ESSes is presented in [11] for reducing overall energy consumption.

In addition to RBE recovery, the utilization of ESSes in a railway system also contributes to line-voltage stabilization and a reduction in the burden of power-feeding systems. As a unique feature of on-board ESS applications, catenary-free operation enables some railway vehicles to operate without an external electricity supply for a certain distance. This capability allows the railway

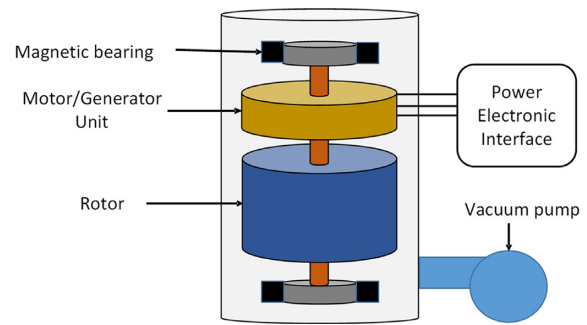


Fig. 1. Schematic diagram of an FESS

vehicle to pass through a zone where overhead line provision is infeasible or where no electrical power supply is present.

In this paper, the fundamentals of these ESS technologies are reviewed in Section 2. A comprehensive comparison of these technologies is made in Section 3. Section 4 presents the main functionalities of railway ESSes with particular applications. In Section 5, the challenges and future trends of railway ESSes are briefly discussed.

2. Fundamentals of railway ESSes

Today, various forms of ESSes—such as flywheels, electric double-layer capacitors (EDLCs), batteries, fuel cells and superconducting magnetic energy storage (SMES) devices—have been proposed and utilized in railway systems for different purposes. These ESSes have their own pros and cons due to the different working principles and material characteristics. Therefore, a clear understanding of the fundamentals of these ESSes is necessary.

2.1 Flywheel

Generally, a flywheel energy storage system (FESS) contains four key components: a rotor, a rotor bearing, an electrical machine and a power electronics interface [12]. The schematic diagram of a FESS is presented in Fig. 1. A FESS converts electrical energy to kinetic energy and stores the mechanical energy in a high-speed rotor, which is connected to an electrical machine via a bearing; the kinetic energy is then converted to electrical energy when necessary.

The rotor of a FESS is mounted in a vacuum or very low-pressure containment in order to eliminate or minimize friction loss [13, 14]. The effects of rotor geometry on the performance of FESSes were studied in [15–17]. Material tensile strength is another factor that determines the maximum

rotational speed of a rotor, since the centrifugal force is proportional to the squared rotational speed [18]. The adoption of high tensile-strength composite materials allows FESSes to operate at a higher rotational speed [19]. Since the characteristics of the rotor materials have a major impact on the flywheel performance, different approaches have been proposed for selecting the proper materials for flywheels [20, 21].

Modern high-speed FESSes cannot adopt conventional mechanical bearings due to the high friction generated, which leads to significant energy loss [13]. As a consequence, mechanical bearings require lubrication in order to minimize friction, and periodic maintenance is inevitable [22]. Alternatively, magnetic bearings have almost no friction due to the benefit of magnetic levitation. Generally, magnetic bearings can be divided into two categories, namely active magnetic bearings (AMBs) and passive magnetic bearings (PMBs). AMBs have high controllability, but the main drawback is the power loss due to the biased current [23]. In contrast, PMBs are based on the utilization of permanent magnets, which means no input power is required [24]. However, the design of PMBs is generally very complex due to the limitation of Earnshaw's theorem [25, 26].

An electrical machine can either perform as a motor when the FESS is charging or operate as a generator when the FESS is discharging. There are various types of electrical machine adopted in FESSes. Generally speaking, electrical machines can be divided into two categories: synchronous and asynchronous machines. The permanent magnet synchronous machine (PMSM) is one of the most popular synchronous machines, which has been widely applied in FESSes due to its high overall efficiency [27]. Since the rotor flux of a PMSM is generated by the permanent magnet, the rotor loss is quite low [12]. High cost and low material-tensile strength are the main disadvantages of PMSMs. Compared with induction machines (IMs), PMSMs are more sensitive to temperature, since the intrinsic coercivity decreases with the increase in temperature [13]. As a typical type of asynchronous machine, IMs are widely used in high-power applications due to their advantages in terms of torque, robustness, construction and cost [22]. However, the rotor design of IMs is more complex, since the rotor requires wires and electric brush connectors [13]. Additionally, speed limitation is another shortcoming of IMs for high-speed FESS applications [28].

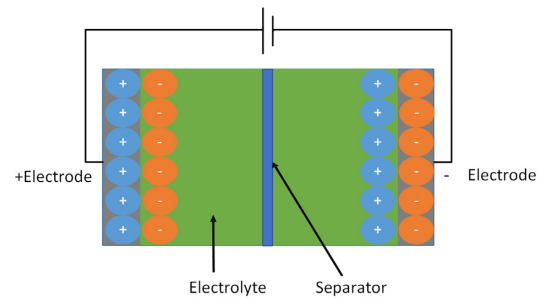


Fig. 2. Schematic diagram of an EDLC

Power electronics technology plays a significant role in energy conversion. A power electronic device provides the appropriate voltage and current for other equipment [29]. Different topologies of power converters have been applied for FESSes, such as DC-AC converters, AC-AC converters, AC-DC-AC converters and their various combinations [30].

2.2 EDLCs

An EDLC contains two electrodes insulated by an ion-permeable separator [31]. Unlike conventional capacitors, the electrodes of EDLCs are soaked in an electrolyte and the capacitance is formed by the accumulated electrostatic charge at the interface between electrode and electrolyte [32], as shown in the schematic diagram in Fig. 2. When an EDLC operates in the charging phase, electrons move from the positive electrode to the negative electrode via the load circuit; this causes the cations and anions in the electrolyte to gather in the negative and positive electrodes, respectively. In the discharging phase, electrons transfer from the negative electrode to the positive electrode via the load circuit and the anions and cations begin to mix again [33].

Generally, the electrodes of an EDLC are usually made of carbon-based materials, since they have high availability and low relative cost. Among different types of carbon-based material used in EDLCs, the most widely used is activated carbon. In addition to low cost, activated carbon materials also have the advantage of a high specific surface area (1000–2000 m²/g) [34]. The activation process can be achieved by a physical or chemical approach at high temperature or by mixing chemicals, respectively [33]. However, due to the poor pore-size control in the activation process, it is difficult to optimize the distribution of pore size in activated carbon materials [34]. Carbide-derived carbon (CDC) is another carbon-based material

used in EDLCs, since the pore size of CDCs can be properly optimized [35]. Generally, CDC-based EDLCs have greater capacitance, since the capacitance is determined by the CDC structure [36]. As a single layer of carbon atoms arranged in a honeycomb crystal lattice, graphene has received much attention in recent years. Graphene-based EDLCs could offer high performance due to their advantages of high cycle capability, flexibility, electrical conductivity and excellent thermal stability [37].

2.3 Batteries

As one of the most commonly used energy-storage devices, batteries store electricity in the form of chemical energy. Generally, a battery contains three key components: the anode, the cathode and the electrolyte. Depending on the chemical material utilized in the electrodes, there are a wide range of batteries. In this section, various battery-based ESSes (BESSes) are introduced, such as lead-acid batteries, nickel-based batteries, sodium-based batteries, lithium-ion batteries and redox-flow batteries.

2.3.1 Lead-acid batteries. The lead-acid battery was invented in 1859, and is therefore known as the oldest type of rechargeable battery. It was widely utilized in cost-sensitive applications due to the advantages of low cost, high reliability and technological maturity. A typical lead-acid battery contains two electrodes: an anode made of sponge lead and a cathode made of lead dioxide materials. The two electrodes are separated by a separator, which is generally made of a microporous membrane, or an absorbed glass mat to prevent short-circuiting. The electrodes and separator are immersed in the diluted sulphuric acid-based electrolyte. In the discharging phase, the anode and the cathode react with the electrolyte to produce lead sulphate and electrical energy. In contrast, lead sulphate and water react under external electrical energy to form lead and lead oxide. Therefore, the amount and size of the sulphate crystals increase if the lead-acid battery is over-discharged or stored at a very low state of charge (SOC), which makes it very difficult to break up the sulphate crystals in the charging process, and can even cause short circuits [38, 39]. Compared with other types of batteries, lead-acid batteries have low energy density and limited cycle capability [40]. To overcome these issues, a variety of lead-acid batteries have been developed, such as valve-regulated lead-acid batteries, deep-cycle

lead-acid batteries and advanced lead-acid batteries [41, 42]. Another shortcoming of lead-acid batteries is their utilization of toxic material lead, which causes metal pollution of nearby agricultural ecosystems during the manufacturing process and at the disposal stage [43].

2.3.2 Nickel-based batteries. The nickel-cadmium (Ni-Cd) battery was invented in 1899, and enjoyed a high market share as a result of continuous performance improvements until the emergence of nickel-metal hydride (Ni-MH) and lithium-ion batteries [44, 45]. The positive and negative electrodes of a typical Ni-Cd battery are made of nickel hydroxide and cadmium, respectively, and the electrolyte is made of alkaline potassium hydroxide. Ni-Cd batteries have low internal resistance and excellent capability to withstand high charge and discharge rates. In addition, Ni-Cd batteries can work on fast charging mode, since the endothermic reactions occur during the charging process. Compared with other rechargeable batteries, a wider operating temperature window is another advantage of Ni-Cd batteries. However, the 'memory effect' and a high self-discharge rate are the major bottlenecks of Ni-Cd batteries [46]. Additionally, the cell voltage of Ni-Cd batteries is much lower than those of lead-acid and lithium-ion batteries, which means more cells are required to connect in series to achieve a certain voltage level. Each cell may have different self-discharge rates, which increases the difficulty of battery-pack balancing. From the perspectives of health and environmental protection, Ni-Cd batteries may cause environmental hazards due to the use of toxic heavy materials such as cadmium [47].

To overcome the shortcomings of Ni-Cd batteries, Ni-MH batteries have been developed to offer better performance in terms of energy density and cycle capability. The negative electrodes of Ni-MH batteries are made of hydride alloy, so Ni-MH batteries are more environmentally friendly than Ni-Cd batteries. Additionally, the impact of 'memory effect' has been largely reduced. A high self-discharge rate is a major disadvantage of Ni-MH batteries. Although this weakness can be mitigated by using a functional separator, it significantly increases the cost and complexity of manufacturing [48].

2.3.3 Sodium-based batteries. Sodium-based batteries operate by the movement of sodium ions between the positive and the negative electrodes.

Generally, the negative electrodes of sodium-based batteries are made of molten sodium. Various derivatives of sodium-based batteries have been developed using different materials in the positive electrodes and electrolytes. Among the candidates, sodium sulphur (NaS) and sodium nickel chloride (NaNiCl_2) batteries are the most common cells. The positive electrode and electrolyte of a NaS battery are made of molten sulphur and solid beta alumina ceramic, respectively. NaS batteries have high energy and power densities, almost no self-discharge, excellent cycle capability and low cost [49]. However, the main drawback of NaS batteries is a high operational temperature requirement, typically in the range of 300–350°C [50].

The sodium nickel chloride battery is also known as the ZEBRA battery, and was developed in the mid 1980s. ZEBRA batteries have higher cell voltage and better safety features [51], but have a lower energy density than NaS batteries [52]. As a member of the molten-salt battery family, ZEBRA batteries also require a high operational temperature, typically in the range of 270–350°C [53]. To overcome the limitation of high operating-temperature requirement, various room-temperature sodium-based batteries have also been proposed [54–56]. However, research in this area is still in its infancy, and there remains a long way to go in terms of its commercial application.

2.3.4 Lithium-ion batteries. The market share of lithium-ion (Li-ion) batteries has increased rapidly in recent years due to their extensive applications in small electronic devices and electric vehicles (EVs) [45]. The operation mechanism of Li-ion batteries is based on the movement of lithium ions. Lithium ions migrate from the positive electrode to the negative electrode in the charging process and travel back in the discharging process. Compared with lead-acid and nickel based batteries, Li-ion batteries have a higher cell voltage, higher energy density, higher charge efficiency and longer lifespan. Depending on the chemical materials adopted in the electrodes, various of Li-ion batteries have been developed, including lithium cobalt oxide (LCO), lithium manganese oxide (LMO), lithium nickel manganese cobalt oxide (NMC), lithium nickel cobalt aluminium oxide (NCA), lithium iron phosphate (LFP) and lithium titanate (LTO) batteries [57]. According to their characteristics, Li-ion batteries can be generally classified into two categories, namely high-power batteries and high-energy batteries.

LFP batteries and LMO batteries are highly acclaimed for their excellent performance in terms of power density. They both offer relatively high current rate during the discharge process. Especially for LFP batteries, the maximum pulse and continuous discharge currents can reach 10°C and 3°C, respectively. The discharge voltage curve of LFP batteries is quite flat, which allows LFP batteries to provide more stable output power with a certain discharge current over the different SOCs [58]. Additionally, LFP batteries also have higher safety performance and a relatively longer lifespan [59]. However, the main disadvantage of LFP batteries is their relatively low specific energy. Compared with other Li-ion batteries, which have a nominal voltage of around 3.6 V to 3.7 V, the nominal voltage of LFP batteries is only 3.2 V. Another drawback of LFP batteries is the relatively high self-discharge rate compared with other Li-ion batteries, although the self-discharge rate of LFP batteries is much lower than those of lead-acid and nickel-based batteries. In contrast, LMO batteries have higher specific energy and lower self-discharge rate than LFP batteries, but their cycle capability is low [60]. To overcome this problem, LMO batteries are generally used in combination with NMC batteries to enhance the specific energy and cyclability. NMC and NCA batteries are the typical nickel-based Li-ion batteries. Compared with LFP and LMO batteries, NMC and NCA batteries have higher specific energy, but the cost is increased due to the utilization of cobalt material. Depending on the applications, NMC and NCA batteries can be designed as either high-power cells or high-energy cells. Compared with LFP batteries, NMC and NCA have cyclability and relative stability issues [59]. While LTOs have emerged as a promising type of Li-ion battery due to their high power capability and extremely long cycle life [61]. However, the main drawbacks of LTO batteries are their relatively low specific energy and high cost [62].

2.3.5 Redox flow batteries. The redox flow battery (RFB) is an electrochemical energy-storage device that provides electrical energy using two active materials in liquid form. The two active materials are commonly separated by an ion-exchange membrane; reduction and oxidation reactions occur on both sides of the ion-exchange membrane when the fluid is pumped. All-vanadium redox flow batteries (VRFBs), polysulphide/bromine flow batteries (PSFBs) and zinc/bromine flow batteries (ZBFBs) are the most

common and commercially available flow batteries. Compared with the other types of batteries, the main advantages of RFBs are their excellent scalability, long cycle life and independent sizing for energy and power [63]. Moreover, since the electrolytes of RFBs are stored in separate tanks, RFBs present almost no self-discharge phenomena. Due to the special structure design, the cell temperature can be handled easily via electrolyte-flow regulation. However, inappropriate operational temperature causes solution precipitation which reduces RFB performance and accelerates degradation. Therefore, the operating temperature of RFBs is typically limited to 15–35°C [64]. Additionally, although RFBs based ESSes have been utilized at the grid level, RFBs still face big challenges for their utilization in transport applications due to their low energy-density and power-density features [65].

2.4 Hydrogen fuel cells

A hydrogen fuel cell (HFC) is an electrochemical device that produces electricity by combining hydrogen fuel and oxygen. Technically, the HFC itself can only produce but cannot store the electricity. Hence, a HFC is usually equipped with a hydrogen storage system to form a regenerative system. Electrolysis of water is a common approach to producing hydrogen. The produced hydrogen is stored in a pressurized storage system for later use. However, this approach presents low efficiency; the efficiency of the water electrolyser, fuel cell and the combination are 70%, 50% and 35%, respectively [66]. Additionally, the produced hydrogen can only be stored by metal-hydride absorbers or carbon absorbers at moderate temperatures and pressures. Compared with the other types of ESS, HFCs have high energy density and moderate power density. HFCs have distinctive features of being non-toxic and pollution-free. Similar to RFBs, HFCs also have excellent scalability [67]. However, their high cost of manufacture and low discharge efficiency, as well as concerns about operational temperature compatibility, severely limit the adoption of fuel cells [68].

2.5 SMESs

SMESs store energy in a magnetic field created by the flow of DC current in the superconducting coil. In order to maintain the superconducting state, the coil is immersed in liquid helium and

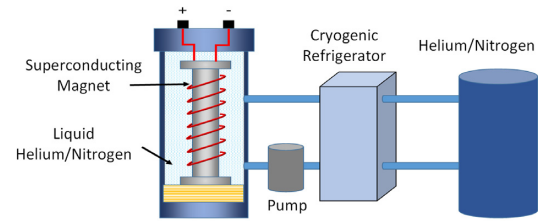


Fig. 3. Schematic diagram of an SMES

cooled to a cryogenic temperature, which should be lower than its superconducting critical temperature [69]. Therefore, a refrigerator is necessary to keep the superconducting coil operating under the cryogenic temperature. The schematic diagram of an SMES is shown in Fig. 3. Since the resistance of the coil is almost zero in its superconducting state, the resistive loss is negligible. Therefore, when the SMES is charged, the electrical energy is converted to magnetic energy, which can be stored in the magnetic field indefinitely. The magnetic energy can be stored indefinitely because there is no degradation of the coil current. When the SMES is required to deliver energy to the external load, the stored magnetic energy is converted to electrical energy by discharging the superconducting coil. Recent progress in this area includes the utilization of high-temperature superconducting materials in order to offer higher performance and economic advantages [70]. Compared with the other types of ESS, SMESes have high energy efficiency, high power density, excellent fast charging/discharging performance and extremely long cycle life (almost infinitely) [71, 72]. The main drawbacks of SMESs are their high cost and the generation of enormous electromagnetic forces when they are utilized as a massive energy-storage device [66].

2.6 Hybrid energy-storage systems

The key idea of a hybrid energy-storage system (HESS) is that heterogeneous ESSes have complementary characteristics, especially in terms of the power density and the energy density [73]. The hybridization synergizes the strengths of each ESS to provide better performance rather than using a single type of ESS. In railway applications, an HESS is generally an integration of at least two types of ESS device, one for high energy demand and one for high power requirements. The high-energy device can be used as an energy supplier to meet long-term energy needs, while the high-power device can be used as a power supplier

to satisfy short-term high power demands. Batteries and fuel cells are ESS devices that can be integrated into an HESS to meet the energy requirements in railway systems. Flywheels, EDLCs, batteries and SMESes are also candidates for forming an HESS. It should be noted that battery ESS devices can serve as either an energy supplier or a power supplier due to their distinctive features. The advantages of various ESSes in railway applications are described and compared in detail in Section 3.

In order to integrate two ESS devices as a single power source, various HESS configurations have been proposed. They can generally be classified into three categories, namely passive parallel, cascade and active [73]. In passive parallel configuration, the two ESS devices are connected without any power electronic device. Although this architecture is simple and easy to implement, the output voltage varies in the charge and discharge stages [38]. The cascade configuration is more efficient than the passive parallel one, but is more expensive to build and employs an additional converter between the ESSes. The ESS devices are therefore decoupled and active energy management can be achieved. However, this configuration lacks the freedom of a control strategy [73] and is restricted by its scalability issues [74]. The active parallel configuration has the highest level of flexibility; each ESS device is connected to a dedicated power converter. Therefore, each ESS device can operate at its optimal conditions and maximum power-point tracking can be achieved [38].

Energy-management strategies are indispensable in the design of HESSes. Energy-management strategies for HESS can be generally grouped into three categories: rule-based, optimization-based and AI-based [75]. Rule-based strategies are widely used in practice due to their simplicity and easy implementation. The rules can be fixed rules or fuzzy rules. Fixed rules are often based on the HESS parameters, while fuzzy rules are generally set based on experience [76]. Optimization-based strategies use optimization algorithms to achieve the optimal power distribution. The most popular strategies include dynamic programming (DP), sequential quadratic programming (SQP), genetic algorithms and Pontryagin's minimum principle (PMP). Most AI-based strategies rely on the mining of system data containing information such as the states of the HESSes, road conditions, driving behaviours and so on. To guarantee reliability, AI-based strategies generally require a large amount of data.

3. ESSes in railway systems

In this section, the main characteristics of different railway ESSes are compared in terms of energy density, power density, cycle efficiency, self-discharge, storage duration, service life, capital cost and environmental impacts.

3.1 Energy density and power density

Gravimetric energy density and gravimetric power density are also known as specific energy and specific power, and they are used to present the total energy and power that an ESS can hold per unit mass. An ESS with high specific energy (or specific power) can store a given amount of energy (or power) with lighter weight. On the other hand, volumetric energy density and volumetric power density are terms used to determine the total energy and power that an ESS can hold per unit volume. Therefore, energy-storage devices with high energy density and power density are suitable for applications where weight and size are among the main considerations. This feature is more important for on-board applications than for stationary applications. For instance, the weight of a railway vehicle increases if an on-board ESS is installed, and therefore the railway vehicle requires more power to meet the traction performance. An inappropriate ESS selection (e.g. low specific energy) leads to low energy efficiency. On the other hand, the size of an on-board ESS is restricted due to safety requirements and economic constraints. According to Table 1, EDLCs have very high gravimetric and volumetric power density, which makes them more competent in high-power applications. Flywheels, Ni-MH batteries, Li-ion batteries and SMESes also have relatively high power density and are widely utilized in power-delivery applications. Generally speaking, battery-based ESSes and HFCs have higher energy densities than other ESSes, which are more suitable for high energy-requirement applications. Depending on the chemical materials used, Li-ion batteries can be designed as either high energy-density products or high power-density products, but not both [88, 89].

3.2 Cycle efficiency

Cycle efficiency, also known as round-trip efficiency, is the ratio of the output electrical energy to the input electrical energy as a percentage during a full charge/discharge cycle. Therefore, it is

Table 1. Comparison of energy and power densities of ESS systems

Technology	Gravimetric energy density (Wh/kg)	Gravimetric power density (W/kg)	Volumetric energy density (Wh/L)	Volumetric power density (W/L)	Reference
Flywheel	5–100	400–1500	20–80	1000–2000	[50, 77]
EDLC	5–15	5000–10 000	10–30	>100 000	[50, 78]
Lead-acid	30–50	75–300	50–90	10–400	[50, 79]
Ni-Cd	50–75	150–300	60–150	75–700	[50, 80]
Ni-MH	54–120	200–1200	190–490	500–3000	[51, 81, 82]
NaS	150–240	150–230	150–250	140–180	[50, 83]
ZEBRA	100–120	150–200	150–180	220–300	[50]
Li-ion	150–250	500–2000	400–650	1500–10,000	[77, 83, 84]
VRFB	10–30	166	25–35	< 2	[50, 83, 85, 86]
HFC	800–10 000	5–800	500–3000	>500	[50, 87]
SMES	0.5–5	500–2000	0.2–2.5	1000–4000	[50, 83]

Table 2. Additional characteristics of ESSes utilized in railway systems

Technology	Cycle efficiency (%)	Daily self-discharge (%)	Typical storage duration	Lifetime (years)	Cycle life (cycles)	Reference
Flywheel	90–95	100	seconds–minutes	20	>21 000	[50, 90]
EDLC	90–97	10–20	seconds–hours	10–30	>100 000	[50, 91]
Lead-acid	80–90	0.05–0.3	minutes–days	5–15	500–2000	[92]
Ni-Cd	60–83	0.2–0.6	minutes–days	15–20	1500–3000	[51, 77]
Ni-MH	65–70	1–2	minutes–days	15–20	1500–3000	[51]
NaS	75–90	15–20	seconds–hours	10–20	2000–4500	[82, 93]
ZEBRA	90	10–15	minutes–hours	10–20	>2500	[50, 82]
Li-ion	90–98	0.1–0.3	minutes–days	8–15	1000–10 000	[50, 82]
VRFB	75–80	0–10	hours–months	10–20	>16 000	[82]
HFC	20–50	Almost zero	hours–days	5–15	>1000	[50]
SMES	94–97	10–15	minutes–hours	>20	>100 000	[50]

a key indicator of energy efficiency. According to [50], the cycle efficiency of ESSes can be classified into three levels: very high efficiency (greater than 90%), high efficiency (60% to 90%) and low efficiency (lower than 60%). As shown in Table 2, Flywheel, EDLC, SMES and Li-ion batteries are among the very high efficiency ESSes. Almost all batteries (in addition to Li-ion batteries) belong to high-efficiency ESSes. Finally, HFCs are the only ESSes listed in this paper that have low efficiency. It is clear that almost all the ESSes utilized in railway systems have very high or high cycle efficiency.

3.3 Self-discharge and storage duration

Self-discharge is the ratio of the dissipated energy to the total amount of stored energy over a certain storage period. It is a critical factor in determining the storage duration of ESSes. Generally, the maximum storage duration increases with a decrease in the self-discharge rate. Depending on the operation frequency, railway systems have different requirements for ESS storage duration. Table 2 illustrates the daily self-discharge

and typical storage duration for railway ESSes. It can be seen that flywheels have the highest self-discharge rate, which leads to a very short storage duration. EDLCs, Na-S batteries, ZEBRA batteries and SMESes also have high self-discharge rates, with a typical storage duration of less than one day. It should be noted that since some ESSes, such as Na-S batteries, ZEBRA batteries and SMESes, operate at very high or low levels of temperature, using the stored energy to maintain the operating temperature is the major reason for their high self-discharge rate. Battery-based ESSes (except Na-S and ZEBRA batteries) generally have lower self-discharge rates, and they are more suitable for long-term energy-storage applications.

3.4 Lifetime

The lifetime of an ESS is generally determined by two factors, namely the cycle life and calendar life. Lifetime is a major factor to consider in applications where the replacement of ESSes is difficult or unacceptable. On the other hand, an ESS that has a short lifetime may also increase the overall

Table 3. Other features of ESSes utilized in railway systems

Technology	Energy capital cost (\$/kWh)	Power capital cost (\$/kW)	Environmental impact	Reference
Flywheel	1000–5000	250–350	Almost none	[50]
EDLC	300–2000	100–300	Slight	[50]
Lead-acid	50–100	200–650	Serious	[77, 94]
Ni-Cd	200–1000	350–1000	Serious	[94]
Ni-MH	240–1200	420–1200	Medium	[90]
NaS	300–500	1000–3000	Slight	[50]
ZEBRA	100–200	150–300	Slight	[50]
Li-ion	273–1000	900–1300	Slight	[50, 77, 95]
VRFB	150–1000	600–1500	Medium	[50]
HFC	~15	~500	Slight	[67, 96]
SMES	1000–10 000	200–300	Medium	[50]

investment cost due to the need for replacements. ESSes that store energy in the form of mechanical (flywheel), electrical (EDLC) or electromagnetic (SMES) energy generally have a long cycle life. Especially for EDLCs, their extremely high cycle life enables them to be cycled frequently over a long period. In contrast, ESSes that store energy in the form of chemical and electrochemical energy, such as HFCs and batteries, generally have a limited cycle life. Additionally, calendar ageing also has a greater impact on chemical and electrochemical energy-based ESSes due to the degradation of their chemical properties.

3.5 Capital cost

For practical applications, capital cost is one of the most critical factors in determining the commercial viability of an ESS. Although some ESSes have excellent performance, they are not economically viable in railway applications due to the excessive capital costs. Furthermore, high capital costs also result in long payback issues. Table 3 summarizes the capital costs in terms of energy and power for ESSes used in railway applications. It can be seen that flywheels, EDLCs and SMESes have a lower capital cost per unit power, and are therefore more suitable for high-power applications. Most batteries and HFCs have a relatively low capital cost per unit energy but a high cost per unit power; they are more suitable for high-energy and long-duration applications. Although lead-acid batteries have a relatively low capital cost, they may not offer the least expensive overall cost due to their limited lifespan. Furthermore, it is worth noting that due to technology breakthroughs and improvements in the supply chain, the prices of some ESSes will drop significantly in the future. According to the estimation in [95], the capital cost of Li-ion batteries may fall to \$74/kWh by 2030.

3.6 Environmental impact

Environmental impact is another key factor in determining if an ESS can be utilized in large-scale applications. It is widely recognized that flywheel-based ESSes are environmentally friendly, since they store energy in kinetic form and do not contain hazardous or toxic metals [97]. EDLCs are also environmentally friendly, since they are made of non-toxic materials. However, it is worth noting that some supercapacitors (especially for pseudocapacitors) may have some environmental issues due to the use of toxic materials in their electrodes and electrolytes, such as the utilization of acetonitrile electrolyte and amorphous hydrous RuO₂-based electrodes [31]. The major environmental issue of batteries is their utilization of toxic materials, especially for lead-acid and Ni-Cd batteries. For SMESes, when the generated electromagnetic force reaches a certain level, it will be harmful to the human body and other organisms [66]. HFCs operate by oxidizing molecular hydrogen, with almost no other by-products other than water. However, HFCs still have a slight impact on the environment due to their generation of hydrogen [98] and their molecular hydrogen emissions [99].

4. Applications of ESSes in railway systems

The applications of ESSes in railway systems can be divided into two categories, namely stationary applications and on-board applications. A stationary ESS—also referred to as a way-side ESS—is generally placed in existing substations or at the track-side where the feeding line has significant voltage fluctuations. An on-board ESS—also known as a mobile ESS—is mounted on a railway vehicle. Generally, a stationary ESS can provide energy for multiple trains from a fixed location. An on-board ESS can only serve the

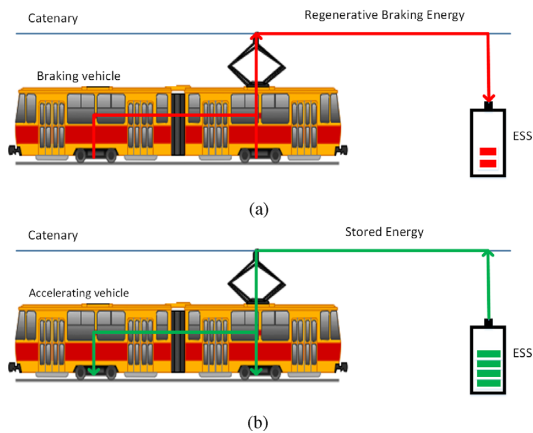


Fig. 4. Operation schematic of a stationary ESS in a railway system: (a) Energy recovery in braking phase; (b) Energy delivery in traction phase

vehicle on which it is mounted but at any location where it is needed. However, since an on-board ESS travels with the railway vehicle, the restrictions on its size and weight are more stringent. Depending on various operational features and demands, both approaches have been widely utilized. On the other hand, the applications of ESSes in railway systems can also be grouped into three categories depending on their functionality, namely RBE recovery, line-power management and catenary-free operation.

4.1 Regenerative braking energy recovery

Both stationary and on-board ESSes can be used to recover RBE and they perform based on the same mechanism. When a railway vehicle is braking, the induction motors in the vehicle function as generators that convert the kinetic energy into electrical energy. The produced RBE is transmitted to and stored in a stationary or on-board ESS. The operation schematic of a stationary ESS is shown in Fig. 4. Generally, the ESS operates in the charging mode when it absorbs the RBE. When the terminal voltage or SOC of the ESS rises to a certain value, the ESS stops charging and stores the injected energy for later use. The ESS acts in discharging mode when it delivers stored energy to the traction vehicles until the terminal voltage or SOC decreases to a certain level. Various ESSes have been proposed or commercially utilized for RBE recovery in railway systems.

As an early application of FESS to recover RBE, a stationary FESS with 2 kW rated power and 25 kWh rated energy was installed at the Zushi station in Japan by the Keihin Electric Express railway in 1988. The FESS achieved 12% energy-saving

performance [100]. In [101, 102], another application of stationary FESS in metro systems was discussed. A FESS with 2 MW rated power and 8.33 kWh rated energy has been installed on the Red Line of the Los Angeles metro system to recover the RBE. Each charge/discharge time is 15 seconds and it completes a full charging/discharging cycle every 1.25 mins. This FESS has achieved 10% to 18% daily energy saving and the expected service life of this FESS can reach over 20 years. On the other hand, FESSes have also been proposed for on-board applications for recovering the RBE. In [103], an on-board FESS in a light rail transit system was investigated; the results suggested that 31% energy savings can be achieved when a 725 kW, 2.9 kWh FESS is mounted in a light rail vehicle (LRV).

EDLCs are one of the most widely utilized ESSes for RBE recovery. In 2002, a stationary EDLC ESS (SITRAS SES) was commissioned near the Ventas station in Madrid. The EDLC ESS was designed to store up to 1 MW power and 2.3 kWh energy [104, 105]. The test result of the EDLC ESS shows that it reduced power consumption per train by 30% and saved 320 MWh energy consumption per year [104]. In 2007, two EDLC ESSes were installed in the Agano substation and the Shomaru substation in Japan. Each EDLC ESS had 288 units (each EDLC unit contains 70 cells) of EDLCs, which were connected as 8 in series and 36 in parallel [100]. The regenerative energy stored in the two systems was 7.7 kWh in total, the energy discharged was 5.9 kWh, and the efficiency of reusing regenerative energy was about 77% [106]. Similarly, EDLC ESSes have also been widely used on-board to recover RBE. In 2003, Bombardier Transportation installed the MITRAC Energy Saver system on a prototype LRV of the MVV Verkehr AG company. According to [107], the MITRAC energy saver system contained 640 EDLC cells, which were arranged as 160 cells connected in series and 4 in parallel. The maximum power and installed energy of the MITRAC Energy Saver were 300 kW and 850 Wh, respectively. The test results indicated that it was able to achieve energy savings of 30%. In 2005, the Central Japan Railway Company installed two EDLC ESSes under the floor of a Series 313 rolling stock. Each EDLC on-board unit had an installation capacity of 0.28 kWh, and it was established by 570 cells connected in series. For each EDLC cell, the operating voltage, capacity and weight were 2.5 V, 800 F and 190 g, respectively. The test results revealed that with one 0.28 kWh EDLC ESS installed on-board, 8% of regenerative energy from the motor was

recovered [108]. In [109], a RBE recycling method for a high-speed railway system using a stationary ESS was proposed. The ESS consisted of three key parts, an EDLC, an energy-storage converter and a back-to-back converter. The energy-storage converter was connected between the DC bus and the EDLC for energy delivery. The back-to-back converter was connected to the isolated transformers to transfer the energy between the two power phases and the EDLC. Isolated transformers were employed to connect the ESS to the traction power system. According to load conditions of the traction power system and SOC limits of EDLC, the ESS has four operation modes, namely charge mode, discharge mode, transfer mode and standby mode. A master-slave control strategy with a central controller was developed for coordinating the operation of the multiple converters.

Among a range of batteries, Li-ion batteries are one of the most popular types used for RBE recovery. In 2005, a verification test of a Li-ion battery-based ESS was carried out in the Myodani substation of the Seishin-Yamate Line in Japan by the Kobe Municipal Transportation Bureau. This operational section demanded a high-energy stationary ESS, since it had an average slope of 2.9% over 4 km [100]. In 2007, the actual system was installed in the Itayado substation. The rated capacity of the actual system was twice as large as the one used in the verification test, and it saved more than 310 MWh energy per year [100]. According to [110], a Li-ion battery-based stationary ESS was installed at the HAIJMA substation in Japan in 2013. The rated capacity, voltage and current of this ESS were 76.12 kWh, 1650 V and 1200 A, respectively. The verification results indicated that the ESS could save more than 5% of total traction power and that about 400 MWh energy could be recovered every year. In 2007, Ni-MH battery-based on-board ESSes were installed and tested on a SWIMO LRV in Japan. According to [111], the ESS module contained 30 cells, which were connected in series to offer a terminal voltage of 36 V and a capacity of 200 Ah. The total weight of the ESS module was 235 kg (including covers and cooling fans), accounting for less than 1% of the total mass weight of the tested train with three car-bodies. The test results revealed that the ESS achieved a 6% increase in energy efficiency. According to [112], a verification test of a Ni-MH battery-based stationary ESS was carried out by the New York City Transit Authority in 2010. This ESS contained four parallel connected units, each of which held 17 modules connected in series. The total voltage, rated

capacity and energy capacity of this ESS were 670 V, 600 Ah and 400 kWh, respectively. The verification results indicated that utilization of the ESS achieved 2.19 times more energy recovery and that 71.4% of the regenerative energy could be stored by the ESS for supplemental use. A VRFB-based on-board ESS solution for RBE recovery was analysed in [65]. Although VRFBs can offer some distinctive features in comparison with other conventional batteries, they are still impractical for commercial applications due to limitations of flow rate, energy density, power density and operational cost [65].

4.2 Line-power management

The ESS also plays a critical role in line-power management in railway systems. Line voltage increases when external energy (such as RBE) is injected to the line powering the same load, while the voltage drops significantly when the supply of power is insufficient to meet the demand from the traction load. The instability of the line voltage not only brings various hazards to the power system but may also cause a power-system failure. Adopting ESSes in the railway system to reduce peak power demands and absorb excess power is one of the mainstream solutions to this problem.

According to [104], a stationary FESS including three high-speed (37 800 rpm) carbon fibre flywheel units connected in parallel was installed in the Northfields substation of the London Underground's Piccadilly Line in 2000. The nominal line voltage of this location was 630 V, and a 180 V voltage drop occurred in the event of a large traction load. The objective of utilizing this FESS was to reduce the line-voltage drop. The test results indicated that with the same load, the line voltage drop was reduced from 180 V to 100 V. Additionally, although the main function of this FESS was to reduce the line-voltage drop, it also contributed to RBE recovery.

In [113], an EDLC-based stationary ESS was proposed in order to compensate for the voltage drop in weak transportation networks. The test results of a reduced size prototype indicated that the voltage drop could be reduced from 58 V to 42 V. In [107], it is shown that the application of a MITRAC energy saver on the prototype LRV not only contributed to energy saving, but also reduced the vehicle peak power demand from the line by up to 50%. In 2010, an EDLC-based ESS was installed in the Daedong substation in Korea. According to [114], the EDLC-based ESS contained 192 modules arranged as 24 modules connected in series and

8 modules connected in parallel. For each module, the capacity and maximum voltage were 165 F and 48.6 V, respectively. The test results revealed that with the utilization of this ESS, the voltage fluctuation was reduced from $\pm 19\%$ to $\pm 6\%$.

In 2006, a Li-ion battery-based stationary ESS was installed in the Shin-Hikida substation in Japan by the West Japan Railway Company. The preliminary purpose of this ESS was to compensate for the short-term line-voltage drop when the power line between Nagahama and Tsuruga was converted from a 20 kV, 60 Hz AC power supply to a 1.5 kV DC power supply [115]. In addition to voltage compensation, this ESS also achieved a daily energy saving of 300 kWh [116]. In [117], a Li-ion battery-based stationary ESS was proposed in order to reduce the voltage drop and peak current of a 3 kV railway power supply line. The terminal voltage, nominal capacity and maximum power of the proposed ESS were 2000 V, 500 kWh and 2000 kW, respectively. Based on the case study of a real 3 kV railway system in Italy, the simulation results showed that the Li-ion battery-based stationary ESS was able to reduce the peak current, voltage drop and losses by 43.2%, 5.26% and 22.4%, respectively. Moreover, for the application of an Ni-MH battery-based stationary ESS in the New York City transit system [112], the ESS could not only capture the RBE, but also stabilize the voltage of the third rail; the voltage drop of the third rail was reduced from 118 V to 63 V with the same load. According to [118], a HESS combining a SMES and a flow battery was proposed to compensate for the power-demand fluctuations caused by high-speed train operations. The SMES was used to suppress high-frequency fluctuations of the traction power demand, while the flow battery was used to compensate for the low-frequency fluctuations. The simulation results revealed that the maximum power fluctuation was reduced by more than 50%.

4.3 Catenary-free operation

Due to difficult construction conditions and the limitations of urban space, the catenary-free operation of railway vehicles has attracted substantial attention. Third rail or ground-level power supplies are also among catenary-free technologies, but in this paper, 'catenary-free' mainly refers to autonomous electric traction. Therefore, stationary ESSes are not within the scope of this section. The on-board ESS must be charged to a certain level of SOC before it can be used for catenary-free

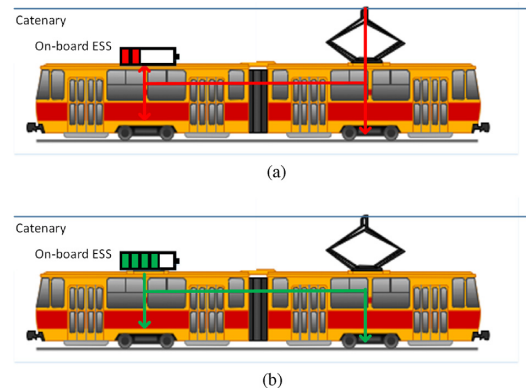


Fig. 5. Schematic diagram of on-board ESS operation: (a) Under catenary operation; (b) Catenary-free operation

operation. As shown in Fig. 5a, when the railway vehicle operates on external power supply, the catenary not only supplies power to the traction system and auxiliary equipment but also charges the on-board ESS. In addition to the catenary, the ESS also can be charged using the RBE when the railway vehicle slows down or approaches the passenger stations. When the railway vehicle runs without external power supply, the on-board ESS operates in discharge mode to power the traction system and auxiliary equipment, as shown in Fig. 5b. The on-board ESS will be recharged when the external power supply is available. High-energy ESSes are generally adopted in this application in order to achieve a long catenary-free distance, and high-power ESSes are utilized to quickly accelerate the vehicles. Nowadays, various ESSes are commercially available for LRVs and trams for catenary-free operation, since they are relatively lightweight and operate at moderate speed.

Almost all the ESSes utilized for catenary-free operation are also considered for recapturing the RBE. For example, the installation of a MITRAC Energy Saver not only aims to recover the RBE but also enables the LRV to carry out catenary-free operation. Authors in [107] showed that a 500 m catenary-free operation was achieved by the LRV with a maximum speed of 26 km/h. In [119], a demonstration of an EDLC-based on-board ESS is reported. This ESS contained 48 modules of EDLCs; the capacity and nominal voltage of each module were 130 F and 54 V, respectively. This ESS was mounted on the roof of a PATP Citadis tram on the RATP T3 line in Paris. The test results showed that a 300 m-long catenary-free operation could be achieved successfully with the adoption of this 1.6 kWh on-board ESS.

According to [120, 121], the Alstom transport company installed Ni-MH battery-based ESSes on the roofs of Citadis trams in Nice, France. Each ESS unit contained 408 Ni-MH cells connected in series, and the rated capacity and nominal voltage of the each cell were 34 Ah and 1.2 V, respectively. The tram equipped with this ESS was able to travel through two catenary-less sections (4.5 and 485 m) at a maximum speed of 30 km/h. A catenary-free operation concept for a Bombardier Flexity 2 tram integrated with a Li-ion based ESS was presented in [122]. The trams have been in service in the Chinese metropolis of Nanjing since 2014; about 90% of the service route implements catenary-free operation, and the maximum catenary-free operation distance reaches 1.38 km. Additionally, a long-distance catenary-free operation test was conducted; the results showed that a 41.6 km catenary-free operation could be achieved with an average speed of 24.7 km/h [122]. In 2016, 19 Avenueio trams were put into operation in Education City, Doha, Qatar. The network has 25 stops on an 11.5 km track without the installation of overhead lines. The trams were powered by the Sitras HES system produced by Siemens. The Sitras HES system is a hybrid energy-storage system for rail vehicles that combines EDLCs and traction batteries. The EDLCs could be recharged at each stop with a 1000 A current and needed only 20 seconds for a full charging process [123].

5. Discussions

Nowadays, although several ESS technologies have been commercially utilized in different applications around the world, some challenges must be overcome before the widespread implementation of railway ESSes can be realized. From an engineering point of view, how to use ESSes more efficiently and more economically is always a complex and challenging issue. A large number of ESS applications have been reported for subway, tram and LRV systems, yet there are still no commercially viable solutions for the use of ESSes in high-speed railway systems. Moreover, with the rapid development of renewable energy technologies, the utilization of renewable energy sources in railway systems with the ESS applications has become a research hotspot.

5.1 ESS selection

For a specific application, choosing the right energy-storage system is essential. As mentioned

in Section 4, a comparative analysis of the characteristics of different ESS technologies is required. ESSes such as flywheels and EDLCs are highly recommended for high-power applications, such as RBE recovery and line-power compensation. As high-energy-density ESSes, batteries are highly favoured for applications in which a certain amount of energy needs to be absorbed or delivered with limited space and weight. Additionally, due to their capacity for long storage duration, batteries are also widely utilized as uninterruptible power sources (UPSs) in railway systems, such as backup power sources for signalling, lighting, ventilation and communication, and so on. It is worth noting that no single ESS can meet the requirements for all applications. Therefore, HESSes are favoured in order to meet various requirements in terms of energy density, power density, operation efficiency, cost of investment and so on.

5.2 ESS sizing

A clear and accurate understanding of the energy and power absorption/delivery requirements is the first step for optimizing the size of an ESS, since the lifetime of some ESSes, such as batteries, depends on the operation depth of discharge (DOD) and charging/discharging rate, and these two parameters are directly determined by the capacity of the ESS. However, as the size of the ESS increases, the corresponding capital and maintenance costs will also increase. An appropriate size not only allows an ESS to perform its duty with better performance, but also contributes to prolonging the life of the ESS and reducing the investment cost. High energy efficiency is another objective that should be considered when optimizing the ESS size, especially for on-board applications. If the ESS is too large, it will increase the overall mass weight of the vehicle, which leads to greater energy consumption in traction. If the ESS is too small, on the other hand, the energy recovered will be limited. Therefore, the overall energy efficiency will be decreased if the size of the ESS is not properly chosen. ESS sizing optimization also includes the selection of suitable proportions for different HESS devices. Different ESS sizing-optimization techniques in railway applications can be found in [124–127].

5.3 ESS location

It is necessary to determine the most suitable location for a stationary ESS in order to achieve

higher energy efficiency and economic payback. The installation location of stationary ESS installations can be divided into two categories, namely at the track side and inside existing traction substations. Generally, the ESSes located at the track side are designed for line-power management, such as line-voltage stabilization and peak power shaving, especially for metro systems [128]. In addition to voltage stabilization, ESSes installed inside substations also aim to enhance energy saving [124]. In order to find the most suitable installation location for an ESS, various optimal objectives should be considered, such as the cancellation of regenerative braking, the energy consumption of the vehicle traction, the total energy loss of the power network, line-voltage fluctuations, the cost of investment and so on. Various optimization methods for ESS location in railway systems are proposed in [124, 125, 129, 130].

5.4 ESSes in high-speed railway systems

Most reported ESS applications for RBE recovery are focused on trams and LRVs. Compared with trams and LRVs, high-speed trains are heavier and run at higher speed. Therefore, a large amount of RBE can be recovered from frequent braking within short periods. Shorter investment payback is another factor that has to be investigated [131]. In [132], it was shown that significant energy savings could be achieved with the utilization of stationary ESSes in high-speed train applications. In [10], two different simulation models of a high-speed train system with an ESS application were developed, and a feasibility analysis was conducted, considering both energy-saving performance and cost effectiveness. Moreover, an energy-management strategy for Li-ion battery-based stationary ESSes was proposed in [133] for the purposes of absorbing peak current and recovering the RBE produced by high-speed trains.

5.5 Integration with smart-grid and renewable energy technologies

The integration of the smart-grid concept in a railway system enables the reuse of the stored RBE for both railway applications and other energy consumers. In [134], a method for using the excess braking energy stored in HESSes to charge hybrid buses was proposed. The smart-grid concept also provides the opportunity for railway ESSes to integrate with renewable energy sources [135]. In [136], the feasibility of implementing a smart grid in a

railway system was analysed, and coordination of renewable energy sources and ESSes was achieved by the proposed supervision strategy. A coordination solution for micro-grid energy management and train-energy consumption was proposed in [137]. An operation methodology based on the utilization of railway ESSes was developed in [138], with the purpose of maximizing both energy savings and cost reduction with the integration of renewable energy sources.

5.6 Economic considerations

Economic considerations play a crucial role in assessing the feasibility of railway ESSes in commercial applications. Reductions in traction-energy consumption contributes to direct energy-cost reduction. Furthermore, energy transmission- and distribution-infrastructure costs are also reduced with the utilization of railway ESSes to recover the RBE [139]. A techno-economic method for sizing ESSes was proposed in [140], with the objective of maximizing the savings in annual energy costs. Except for the cost of energy consumption, large fluctuations in power demand led the railway operator to pay an additional charge. A solution based on the utilization of ESSes was proposed in [141], which confirmed that significant reductions in power demand could be achieved. Moreover, since the catenary-free trams powered by EDLCs require high charging power from the stations, this may cause the local grid to suffer from power superposition when several trams charge at the same time, leading to significant power-quality degradation such as voltage sags and large harmonics injections. In order to reduce charging power superposition, the installation of stationary ESSes to assist in the charging of the trams was proposed in [142]. The trade-off between component cost and operation cost was optimized while taking into consideration ESS type selection, sizing and configuration. The case study results showed that an 11.48% saving in annual costs could be achieved.

6. Conclusions

This paper has presented a comprehensive review of different ESS technologies that can be used in railway systems. The advantages and disadvantages of each ESS technology have been analysed. Both flywheels and EDLCs have been commercially utilized as both stationary and on-board

ESSes in tram and LRV systems. With the rapid development of Ni-MH and Li-ion battery technologies, the application of BESSes in railway systems has received substantial attention in recent years. In addition to their high energy density, significant improvements in power density and cycle life mean that BESSes have great potential for the future. Although HFCs have been commercially utilized in road vehicles (cars and buses), they still have not been widely used in railway systems due to the limitations of low power density, low cycle efficiency and high investment cost. SMESes are commercially utilized in the electrical grid for power-quality control and grid stabilization due to their fast response capability, but their low cost efficiency and high safety requirements (very low temperature and high magnetic operational environment) are major obstacles to their application in railway systems. By combining the distinctive advantages of different energy-storage technologies in a single solution, HESSes may have a greater potential for railway applications in the future. This paper has demonstrated that ESSes can not only improve energy efficiency and power quality but also bring considerable economic returns in railway applications.

Conflict of interest statement. None declared.

References

- Liu L, Hwang T, Lee S, et al. Emission projections for long-haul freight trucks and rail in the United States through 2050. *Environ Sci Technol* 2015; **49**:11569–76.
- Hoffrichter A, Miller AR, Hillmansen S, et al. Well-to-wheel analysis for electric, diesel and hydrogen traction for railways. *Transport R D-Tr E* 2012; **17**:28–34.
- Peña-Alcaraz M, Fernández A, et al. Optimal underground timetable design based on power flow for maximizing the use of regenerative-braking energy. *P I Mech Eng F-J Rai* 2012; **226**:397–408.
- Nasri A, Moghadam MF, Mokhtari H. Timetable optimization for maximum usage of regenerative energy of braking in electrical railway systems. In: *International Symposium on Power Electronics, Electrical Drives, Automation and Motion (SPEEDAM)*, Pisa, Italy, 2010, 1218–21.
- Li X, Lo HK. Energy minimization in dynamic train scheduling and control for metro rail operations. *Transport Res B-Meth* 2014; **70**:269–84.
- Scheepmaker GM, Goverde RM, Kroon LG. Review of energy-efficient train control and timetabling. *Eur J Oper Res* 2017; **257**:355–76.
- Abbas H, Kim Y, Siegel JB, et al. Optimization of energy-efficient speed profile for electrified vehicles. In: *ASME 2018 Dynamic Systems and Control Conference*, Atlanta, GA, USA, 2018, V002T15A006.
- Su S, Tang T, Li X. Driving strategy optimization for trains in subway systems. *P I Mech Eng F-J Rai* 2018; **232**:369–83.
- Bitoleanu A, Popescu M, Suru CV. Configuring and experimental evaluation of a laboratory model for filtering and regeneration in active DC traction substations. In: *10th International Symposium on Advanced Topics in Electrical Engineering (ATEE)*, Bucharest, Romania, 2017, 591–6.
- Ceraolo M, Lutzemberger G, Meli E, et al. Energy storage systems to exploit regenerative braking in DC railway systems: different approaches to improve efficiency of modern high-speed trains. *J Energy Storage* 2018; **16**:269–79.
- Barrero R, Tackoen X, Van Mierlo J. Stationary or onboard energy storage systems for energy consumption reduction in a metro network. *P I Mech Eng F-J Rai* 2010; **224**:207–25.
- Faraji F, Majazi A, Al-Haddad K, et al. A comprehensive review of flywheel energy storage system technology. *Renew Sust Energ Rev* 2017; **67**:477–90.
- Bolund B, Bernhoff H, Leijon M. Flywheel energy and power storage systems. *Renew Sust Energ Rev* 2007; **11**:235–58.
- Suzuki Y, Koyanagi A, Kobayashi M, et al. Novel applications of the flywheel energy storage system. *Energy* 2005; **30**:2128–43.
- Arnold S, Saleeb A, Al-Zoubi N. Deformation and life analysis of composite flywheel disk systems. *Compos Part B-Eng* 2002; **33**:433–59.
- Jiang L, Zhang W, Ma G, et al. Shape optimization of energy storage flywheel rotor. *Struct Multidiscip O* 2017; **55**:739–50.
- Kale V, Secanell M. A comparative study between optimal metal and composite rotors for flywheel energy storage systems. *Energy Rep* 2018; **4**:576–85.
- Genta G. *Kinetic Energy Storage: Theory and Practice of Advanced Flywheel Systems*. Butterworth-Heinemann, London, UK, 2014.
- Tzeng J, Emerson R, Moy P. Composite flywheels for energy storage. *Compos Sci Technol* 2006; **66**:2520–7.
- Patil SS, Bhalerao YJ. Selection of levels of dressing process parameters by using TOPSIS technique for surface roughness of en-31 work piece in CNC cylindrical grinding machine. In: *IOP Conference Series: Materials Science and Engineering*, Orissa, India, 2017, 012033.
- Asodariya H, Patel HV, Babariya D, et al. Application of multi criteria decision making method to select and validate the material of a flywheel design. *Mater Today-Proc* 2018; **5**:17147–55.
- Peña-Alzola R, Sebastián R, Quesada J et al. Review of flywheel based energy storage systems. In: *International Conference on Power Engineering, Energy and Electrical Drives (POWERENG)*, Malaga, Spain, 2011, 1–6.
- Bangcheng H, Shiqiang Z, Xi W, et al. Integral design and analysis of passive magnetic bearing and active radial magnetic bearing for agile satellite application. *IEEE T Magn* 2012; **48**:1959–66.
- Filatov AV, Maslen EH. Passive magnetic bearing for flywheel energy storage systems. *IEEE T Magn* 2001; **37**:3913–24.
- Paden B, Groom N, Antaki JF. Design formulas for permanent-magnet bearings. *J Mech Design* 2003; **125**:734–8.
- Bassani R. Earnshaw (1805–1888) and passive magnetic levitation. *Meccanica* 2006; **41**:375–89.
- Pillay P, Krishnan R. Modeling, simulation, and analysis of permanent-magnet motor drives. I. The permanent-magnet synchronous motor drive. *IEEE T Ind Appl* 1989; **25**:265–73.

28. Daoud MI, Abdel-Khalik A, Massoud A, et al. On the development of flywheel storage systems for power system applications: a survey. In: *20th International Conference on Electrical Machines (ICEM)*, Marseille, France, 2012, 2119–25.
29. Gharehpetian GB, Agah SMM. *Distributed Generation Systems: Design, Operation and Grid Integration*, Oxford, UK., Butterworth-Heinemann, 2017.
30. Amiryar M, Pullen K. A review of flywheel energy storage system technologies and their applications. *Appl Sci* 2017; 7:286.
31. Wang G, Zhang L, Zhang J. A review of electrode materials for electrochemical supercapacitors. *Chem Soc Rev* 2012; 41:797–828.
32. Zhang LL, Zhao X. Carbon-based materials as supercapacitor electrodes. *Chem Soc Rev* 2009; 38:2520–31.
33. González A, Goikolea E, Barrena JA, et al. Review on supercapacitors: technologies and materials. *Renew Sust Energy Rev* 2016; 58:1189–206.
34. Simon P, Burke A. Nanostructured carbons: double-layer capacitance and more. *Elec Soc Interface* 2008; 17:38.
35. Chmiola J, Yushin G, Gogotsi Y, et al. Anomalous increase in carbon capacitance at pore sizes less than 1 nanometer. *Science* 2006; 313:1760–3.
36. Gu W, Yushin G. Review of nanostructured carbon materials for electrochemical capacitor applications: advantages and limitations of activated carbon, carbide-derived carbon, zeolite-templated carbon, carbon aerogels, carbon nanotubes, onion-like carbon, and graphene. *Wires Energy Environ* 2014; 3:424–73.
37. Pumera M. Graphene-based nanomaterials and their electrochemistry. *Chem Soc Rev* 2010; 39:4146–57.
38. Vazquez S, Lukic SM, Galvan E, et al. Energy storage systems for transport and grid applications. *IEEE T Ind Electron* 2010; 57:3881–95.
39. Ruetschi P. Aging mechanisms and service life of lead–acid batteries. *J Power Sources* 2004; 127:33–44.
40. Kreith F, Goswami DY. *Energy Management and Conservation Handbook*, Boca Raton, US, CRC Press; 2007.
41. McKeon BB, Furukawa J, Fenstermacher S. Advanced lead–acid batteries and the development of grid-scale energy storage systems. *P IEEE* 2014; 102:951–63.
42. Moseley PT, Rand DA, Peters K. Enhancing the performance of lead–acid batteries with carbon: in pursuit of an understanding. *J Power Sources* 2015; 295:268–74.
43. Liu G, Yu Y, Hou J, et al. An ecological risk assessment of heavy metal pollution of the agricultural ecosystem near a lead-acid battery factory. *Ecol Indic* 2014; 47:210–18.
44. Putois F. Market for nickel-cadmium batteries. *J Power Sources* 1995; 57:67–70.
45. Pillot C. The rechargeable battery market and main trends 2014–2025. In: *31st International Battery Seminar & Exhibit*, Fort Lauderdale, FL, USA, 2015, 5–7.
46. Reddy TB. *Linden's Handbook of Batteries*, McGraw-Hill Education. New York, 2011.
47. Lacerda VG, Mageste AB, Santos IJB, et al. Separation of Cd and Ni from Ni–Cd batteries by an environmentally safe methodology employing aqueous two-phase systems. *J Power Sources* 2009; 193:908–13.
48. Kritzer P, Cook JA. Nonwovens as separators for alkaline batteries an overview. *J Electrochem Soc* 2007; 154:A481–94.
49. Oshima T, Kajita M, Okuno A. Development of sodium-sulfur batteries. *Int J Appl Ceram Tec* 2004; 1:269–76.
50. Chen H, Cong TN, Yang W, et al. Progress in electrical energy storage system: a critical review. *Prog Nat Sci* 2009; 19:291–312.
51. González-Gil A, Palacin R, Batty P. Sustainable urban rail systems: strategies and technologies for optimal management of regenerative braking energy. *Energ Convers Manage* 2013; 75:374–88.
52. Palacin MR. Recent advances in rechargeable battery materials: a chemist's perspective. *Chem Soc Rev* 2009; 38:2565–75.
53. Dustmann CH. Advances in ZEBRA batteries. *J Power Sources* 2004; 127:85–92.
54. Carter R, Oakes L, Douglas A, et al. A sugar-derived room-temperature sodium sulfur battery with long term cycling stability. *Nano Lett* 2017; 17:1863–9.
55. Kumar D, Kuhar SB, Kanchan D. Room temperature sodium-sulfur batteries as emerging energy source. *J Energy Storage* 2018; 18:133–48.
56. Wang YX, Zhang B, Lai W, et al. Room-temperature sodium-sulfur batteries: a comprehensive review on research progress and cell chemistry. *Adv Energy Mater* 2017; 7:1602829.
57. Liu X, Li K, Li X. The electrochemical performance and applications of several popular lithium-ion batteries for electric vehicles: a review. In: Li K, Zhang J, Chen M, et al. (eds). *Advances in Green Energy Systems and Smart Grid*. Singapore: Springer Singapore, 2018,201–213.
58. Zou Y, Hu X, Ma H, et al. Combined state of charge and state of health estimation over lithium-ion battery cell cycle lifespan for electric vehicles. *J Power Sources* 2015; 273:793–803.
59. Jaguemont J, Boulon L, Dubé Y. A comprehensive review of lithium-ion batteries used in hybrid and electric vehicles at cold temperatures. *Appl Energy* 2016; 164:99–114.
60. Thackeray MM. Manganese oxides for lithium batteries. *Prog Solid State Ch* 1997; 25:1–71.
61. Sandhya C, John B, Gouri C. Lithium titanate as anode material for lithium-ion cells: a review. *Ionics* 2014; 20:601–20.
62. Nitta N, Wu F, Lee JT, et al. Li-ion battery materials: present and future. *Mater Today* 2015; 18:252–64.
63. Wang W, Luo Q, Li B, et al. Recent progress in redox flow battery research and development. *Adv Funct Mater* 2013; 23:970–86.
64. Alotto P, Guarnieri M, Moro F. Redox flow batteries for the storage of renewable energy: a review. *Renew Sust Energy Rev* 2014; 29:325–35.
65. Campillo J, Ghaviha N, Zimmerman N, et al. Flow batteries use potential in heavy vehicles. In: *International Conference on Electrical Systems for Aircraft, Railway, Ship Propulsion and Road Vehicles (ESARS)*, Aachen, Germany, 2015, 1–6.
66. Ibrahim H, Ilinca A, Perron J. Energy storage systems: characteristics and comparisons. *Renew Sust Energy Rev* 2008; 12:1221–50.
67. Luo X, Wang J, Dooner M, et al. Overview of current development in electrical energy storage technologies and the application potential in power system operation. *Appl Energy* 2015; 137:511–36.
68. O'Hayre R, Cha SW, Prinz FB, et al. *Fuel Cell Fundamentals*, Hoboken, US, John Wiley & Sons, 2016.
69. Holla RV. Energy storage methods: superconducting magnetic energy storage: a review. *J Undergrad Res Univ Ill Chic* 2015; 8:49–54.

70. Ren G, Ma G, Cong N. Review of electrical energy storage system for vehicular applications. *Renew Sust Energy Rev* 2015; **41**:225–36.
71. Hall PJ, Bain EJ. Energy-storage technologies and electricity generation. *Energy Policy* 2008; **36**:4352–5.
72. Melhem Z. *High Temperature Superconductors (HTS) for Energy Applications*, Cambridge, UK: Elsevier, 2011.
73. Hemmati R, Saboori H. Emergence of hybrid energy storage systems in renewable energy and transport applications: a review. *Renew Sust Energy Rev* 2016; **65**:11–23.
74. Khaligh A, Li Z. Battery, ultracapacitor, fuel cell, and hybrid energy storage systems for electric, hybrid electric, fuel cell, and plug-in hybrid electric vehicles: state of the art. *IEEE T Veh Technol* 2010; **59**:2806–14.
75. Sun L, Feng K, Chapman C, et al. An adaptive power-split strategy for battery-supercapacitor powertrain: design, simulation, and experiment. *IEEE T Power Electr* 2017; **32**:9364–75.
76. Wang Y, Yang Z, Lin F, et al. A hybrid energy management strategy based on line prediction and condition analysis for the hybrid energy storage system of tram. *IEEE T Ind Appl* 2020; **56**:1793–803.
77. Hadjipaschalis I, Poullikkas A, Efthimiou V. Overview of current and future energy storage technologies for electric power applications. *Renew Sust Energy Rev* 2009; **13**:1513–22.
78. Parfomak PW. Energy storage for power grids and electric transportation: a technology assessment. *Technical report. Congressional Research Service* 2012.
79. Farret FA, Simoes MG. *Integration of Alternative Sources of Energy*, Hoboken, US.. John Wiley & Sons, 2006.
80. Zhao H, Wu Q, Hu S, et al. Review of energy storage system for wind power integration support. *Appl Energy* 2015; **137**:545–53.
81. Fetcenko M, Ovshinsky S, Reichman B, et al. Recent advances in NiMH battery technology. *J Power Sources* 2007; **165**:544–51.
82. Chatzivasileiadi A, Ampatzi E, Knight I. Characteristics of electrical energy storage technologies and their applications in buildings. *Renew Sust Energy Rev* 2013; **25**:814–30.
83. International Electrotechnical Commission. Electrical energy storage: white paper. *Technical report. IEC* 2011.
84. Howard WF, Spotnitz RM. Theoretical evaluation of high-energy lithium metal phosphate cathode materials in Li-ion batteries. *J Power Sources* 2007; **165**:887–91.
85. Barote L, Weissbach R, Teodorescu R, et al. Stand-alone wind system with vanadium redox battery energy storage. In: *11th International Conference on Optimization of Electrical and Electronic Equipment (OPTIM)*, Brasov, Romania, 2008, 407–12.
86. Weber AZ, Mench MM, Meyers JP, et al. Redox flow batteries: a review. *J Appl Electrochem* 2011; **41**:1137–64.
87. Winter M, Brodd RJ. What are batteries, fuel cells, and supercapacitors? *Chem Rev* 2005; **104**:4245–69.
88. Yi TF, Yang SY, Xie Y. Recent advances of Li 4 Ti 5 O 12 as a promising next generation anode material for high power lithium-ion batteries. *J Mater Chem A* 2015; **3**:5750–77.
89. Schipper F, Erickson EM, Erk C, et al. Recent advances and remaining challenges for lithium ion battery cathodes I. Nickel-Rich, LiNi_xCo_yMn_zO₂. *J Electrochem Soc* 2017; **164**:A6220–8.
90. Schoenung SM. Characteristics and technologies for long-vs short-term energy storage. *Technical report. United States Department of Energy* 2001.
91. Pickard WF, Shen AQ, Hansing NJ. Parking the power: strategies and physical limitations for bulk energy storage in supply-demand matching on a grid whose input power is provided by intermittent sources. *Renew Sust Energy Rev* 2009; **13**:1934–45.
92. Battke B, Schmidt TS, Grosspietsch D, et al. A review and probabilistic model of lifecycle costs of stationary batteries in multiple applications. *Renew Sust Energy Rev* 2013; **25**:240–50.
93. Arangarajan V, Oo AMT, Chandran J, et al. Role of energy storage in the power system network. In: Kale SA, Thirumalalai PR, Prabaker K (eds). *Renewable Energy and Sustainable Development*. Hauppauge, NY: Nova Science, 2015, 201–25.
94. Tzimas E, Moss R, Ntagia P. Technology map of the European Strategic Energy Technology plan (SET-Plan). *Technical report. JRC Scientific and Technical Reports* 2011.
95. Curry C. Lithium-ion battery costs and market. *Technical report. Bloomberg New Energy Finance* 2017.
96. Schoenung SM, Hassenzahl WV. Long-vs. short-term energy storage technologies analysis a life-cycle cost study a study for the DOE energy storage systems program. *Technical report. Sandia National Laboratories* 2003.
97. Wicki S, Hansen EG. Clean energy storage technology in the making: an innovation systems perspective on flywheel energy storage. *J Clean Prod* 2017; **162**:1118–34.
98. Edwards PP, Kuznetsov VL, David WI, et al. Hydrogen and fuel cells: towards a sustainable energy future. *Energy Policy* 2008; **36**:4356–62.
99. Tromp TK, Shia RL, Allen M, et al. Potential environmental impact of a hydrogen economy on the stratosphere. *Science* 2003; **300**:1740–2.
100. Okui A, Hase S, Shigeeda H, et al. Application of energy storage system for railway transportation in Japan. In: *International Power Electronics Conference (IPEC)*, Shapporo, Japan, 2010, 3117–23.
101. Solis O, Castro F, Bukhin L, et al. LA metro red line wayside energy storage substation revenue service regenerative energy saving results. In: *Joint Rail Conference of the American Society of Mechanical Engineers*, Colorado Springs, CO, USA, 2014, V001T07A003.
102. Solis O, Castro F, Bukhin L, et al. Saving money every day: LA metro subway wayside energy storage substation. In: *Joint Rail Conference of the American Society of Mechanical Engineers*, San Jose, CA, USA, 2015, V001T07A002.
103. Rupp A, Baier H, Mertiny P, et al. Analysis of a flywheel energy storage system for light rail transit. *Energy* 2016; **107**:625–38.
104. Radcliffe P, Wallace JS, Shu LH. Stationary applications of energy storage technologies for transit systems. In: *Electric Power and Energy Conference (EPEC)*, Halifax, Canada, 2010, 1–7.
105. Maher B. Ultracapacitors provide cost and energy savings for public transportation applications. *Battery Power Prod Technol* 2006; **10**, 1–4.
106. Konishi T, Tobita M. Fixed energy storage technology applied for DC electrified railway (traction power substation). In: *Electrical Systems for Aircraft, Railway and Ship Propulsion (ESARS)*, Bologna, Italy, 2012, 1–6.
107. Steiner M, Scholten J. Energy storage on board of DC fed railway vehicles PESC 2004 conference in Aachen, Germany. In: *35th Annual Power Electronics Specialists Conference*, Aachen, Germany, 2004, 666–71.

108. Sekijima Y, Inui M, Monden Y, et al. Development of an energy storage system for DC electric rolling stock by applying electric double layer capacitors. *Japan Rail Eng* 2006; **46**:35.
109. Chen J, Hu H, Ge Y, et al. An energy storage system for recycling regenerative braking energy in high-speed railway. *IEEE T Power Deliver* 2020, doi: 10.1109/TPWRD.2020.2980018.
110. Hayashiya H, Hara D, Tojo M, et al. Lithium-ion battery installation in traction power supply system for regenerative energy utilization: initial report of effect evaluation after half a year operation. In: *16th International Power Electronics and Motion Control Conference and Exposition (PEMC)*, Antalya, Turkey, 2014, 119–24.
111. Akiyama S, Tsutsumi K, Matsuki S. The development of low floor battery-driven LRV 'SWIMO'. *Journal of the Society of Mechanical Engineers*, 2008; **111**:468–9.
112. Ogura K, Nishimura K, Matsumura T, et al. Test results of a high capacity wayside energy storage system using Ni-MH batteries for DC electric railway at New York City transit. In: *Green Technologies Conference (IEEE-Green)*, Baton Rouge, LA, USA, 2011, 1–6.
113. Rufer A, Hotellier D, Barrade P. A supercapacitor-based energy storage substation for voltage compensation in weak transportation networks. *IEEE T Power Deliver* 2004; **19**:629–36.
114. Lee H, Kim G, Lee C, et al. Field tests of DC 1500 V stationary energy storage system. *Int J Railway* 2012; **5**:124–8.
115. Sone S. Improvement of traction power feeding/regeneration system by means of energy storage devices. In: *Electrical Systems for Aircraft, Railway and Ship Propulsion (ESARS)*, Bologna, Italy, 2010, 1–6.
116. Suzuki T, Hayashiya H, Yamanoi T, et al. Introduction and practical use of energy storage system with lithium-ion battery for DC traction power supply system. *IEEJ J Ind Appl* 2016; **5**:20–5.
117. Lamedica R, Ruvio A, Galdi V, et al. Application of battery auxiliary substations in 3kV railway systems. In: *AEIT International Annual Conference*, Naples, Italy, 2015, 1–6.
118. Suzuki S, Baba J, Shutoh K, et al. Effective application of superconducting magnetic energy storage (SMES) to load leveling for high speed transportation system. *IEEE T Appl Supercon* 2004; **14**:713–16.
119. Moskowitz JP, Coahuau JL. STEEM: ALSTOM and RATP experience of supercapacitors in tramway operation. In: *Vehicle Power and Propulsion Conference (VPPC)*, Lille, France, 2010, 1–5.
120. Ogasa M. Application of energy storage technologies for electric railway vehicles—examples with hybrid electric railway vehicles. *IEEJ T Electr Electr* 2010; **5**:304–11.
121. Rufer A. Energy storage for railway systems, energy recovery and vehicle autonomy in Europe. In: *International Power Electronics Conference (IPEC)*, Sapporo, Japan, 2010, 3124–7.
122. Becker F, Dämmig A. Catenary free operation of light rail vehicles—topology and operational concept. In: *18th European Conference on Power Electronics and Applications (EPE '16 ECCE Europe)*, Karlsruhe, Germany, 2016, 1–10.
123. Guerrieri M. Catenary-free tramway systems: functional and cost-benefit analysis for a metropolitan area. *Urban Rail Transit* 2019; **5**:289–309.
124. Wang B, Yang Z, Lin F, et al. An improved genetic algorithm for optimal stationary energy storage system locating and sizing. *Energies* 2014; **7**:6434–58.
125. Xia H, Chen H, Yang Z, et al. Optimal energy management, location and size for stationary energy storage system in a metro line based on genetic algorithm. *Energies* 2015; **8**:11618–40.
126. de la Torre S, Sánchez-Racero AJ, Aguado JA, et al. Optimal sizing of energy storage for regenerative braking in electric railway systems. *IEEE T Power Syst* 2015; **30**:1492–500.
127. Herrera V, Milo A, Gaztañaga H, et al. Adaptive energy management strategy and optimal sizing applied on a battery-supercapacitor based tramway. *Appl Energ* 2016; **169**:831–45.
128. Suzuki T, Hayashiya H, Yamanoi T, et al. Application examples of energy saving measures in Japanese DC feeding system. In: *International Power Electronics Conference (IPEC-Hiroshima 2014-ECCE-ASIA)*, Hiroshima, Japan, 2014, 1062–7.
129. Ratniyomchai T, Hillmansen S, Tricoli P. Optimal capacity and positioning of stationary supercapacitors for light rail vehicle systems. In: *International Symposium on Power Electronics, Electrical Drives, Automation and Motion (SPEEDAM)*, Ischia, Italy, 2014, 807–12.
130. Ratniyomchai T, Hillmansen S, Tricoli P. Energy loss minimisation by optimal design of stationary supercapacitors for light railways. In: *International Conference on Clean Electrical Power (ICCEP)*, Taormina, Italy, 2015, 511–17.
131. Ceraolo M, Lutzemberger G. Stationary and on-board storage systems to enhance energy and cost efficiency of tramways. *J Power Sources* 2014; **264**:128–39.
132. Frilli A, Meli E, Nocciolini D, et al. Braking energy recovery in high speed trains: an innovative model. In: Boschetti G, Gasparetto A (eds). *Advances in Italian Mechanism Science: Proceedings of the First International Conference of IFToMM Italy*. Cham: Springer International, 2017, 327–34.
133. Calderaro V, Galdi V, Graber G, et al. Energy management of auxiliary battery substation supporting high-speed train on 3 kV DC systems. In: *International Conference on Renewable Energy Research and Applications (ICRERA)*, Palermo, Italy, 2015, 1224–9.
134. Nasr S, Iordache M, Petit M. Smart micro-grid integration in DC railway systems. In: *PES Innovative Smart Grid Technologies Conference Europe (ISGT-Europe)*, Istanbul, Turkey, 2014, 1–6.
135. Şengör İ, Kılıçkiran HC, Akdemir H, et al. Energy management of a smart railway station considering regenerative braking and stochastic behaviour of ESS and PV generation. *IEEE T Sustain Energ* 2018; **9**:1041–50.
136. Pankovits P, Pouget J, Robyns B, et al. Towards railway-smartgrid: energy management optimization for hybrid railway power substations. In: *PES Innovative Smart Grid Technologies Conference Europe (ISGT-Europe)*, Istanbul, Turkey, 2014, 1–6.
137. Novak H, Vašak M, Lešić V. Hierarchical energy management of multi-train railway transport system with energy storages. In: *International Conference on Intelligent Rail Transportation (ICIRT)*, Birmingham, UK, 2016, 130–8.
138. Aguado JA, Racero AJS, de la Torre S. Optimal operation of electric railways with renewable energy and electric storage systems. *IEEE T Smart Grid* 2018; **9**:993–1001.
139. Khodaparastan M, Mohamed AA, Brandauer W. Recuperation of regenerative braking energy in electric rail transit systems. arXiv:1808.05938 [eess.SP], 2018.

140. Graber G, Calderaro V, Galdi V, et al. Techno-economic sizing of auxiliary-battery-based substations in DC railway systems. *IEEE T Transport Electrification* 2018; 4:616–25.
141. Roch-Dupré D, López-López ÁJ, Pecharrmán RR, et al. Analysis of the demand charge in DC railway systems and reduction of its economic impact with energy storage systems. *Int J Elec Power* 2017; 93:459–67.
142. Wei S, Jiang J, Murgovski N, et al. Optimisation of a catenary-free tramline equipped with stationary energy storage systems. *IEEE T Veh Technol* 2020; 69:2449–62.